

RESEARCH

Open Access



# Evaluation of the adsorption behavior and divalent metal ions removal efficiency of ceramic point-of-use water filter materials

Ohene B. Apea<sup>1</sup>, Bennet Edem Akorley<sup>1\*</sup>, Emmanuel O. Oyelude<sup>1</sup> and Boateng Ampadu<sup>2</sup>

## Abstract

Ceramic water filters (CWFs) are point-of-use devices mostly used in developing countries as a result of their effectiveness in the treatment of household water. However, there is a dearth of knowledge on the metal ions adsorption behavior of the filter materials. Therefore, this study investigates the adsorption behavior of the divalent metal ions using commercially available ceramic water filters as adsorbents, in a batch experiment and compared the data, to the extent of metal ion removal during filtration. The ceramic water filters were characterized with x-ray fluorescence spectrometer, x-ray powder diffractometer and fourier-transform infrared spectrophotometer. An adsorption batch experiment was conducted and filtration experiments were performed to determine the extent of divalent metal ions removed. The results of the study showed that divalent metal ions were adsorbed efficiently by ceramic water filters. The pseudo-second-order kinetic model best described the kinetic behavior of metal ion removal process. The extent of adsorption of ceramic water filters was in the range: 7.015–335.77 mgg<sup>-1</sup>. The adsorption patterns fitted the Freundlich isotherm model while the entropy, enthalpy, and Gibbs free energy, indicate that the processes for all CWF-adsorbents are endothermic, feasible and spontaneous. The kinetic and thermodynamic behavior of CWF-adsorbents indicate that the mechanism of the sorption process is chemisorption. There was a significant difference in the amount of divalent metal ions adsorbed in batch experiments compared to filtration experiments for ceramic water filter materials (Pot filter and candle filter). The metal ions adsorption potentials of ceramic water filters are found to be rate dependent; hence the rate of filtration must be of concern to manufacturers.

**Keywords** Ceramic water filters, Adsorption, Point-of-Use, Equilibrium time, Adsorbent dose, Isotherm, Gibbs free energy, Enthalpy change, Endothermic and mechanism

## Introduction

Access to drinking water remains a significant challenge for millions of people around the world. The Joint Monitoring Report by WHO and UNICEF highlights

that approximately 844 million individuals lack access to safe drinking water (WHO 2017). While efforts have been made to expand water supply and quality management in most developing countries, issues such as heavy metal pollution from illegal mining activities, industrial waste disposal, pharmaceutical waste disposal and other sources continue to pose a significant threat to water quality (Shah and Joshi 2017; Whelan et al. 2022).

In addressing these challenges, point-of-use technologies, such as filters have been introduced in most developing countries, with ceramic water filters (CWFs) gaining increasing acceptance in Ghana. The treatment of heavy pollutants in source water requires filter materials

\*Correspondence:

Bennet Edem Akorley  
bennetakorley@gmail.com

<sup>1</sup> Department of Applied Chemistry, School of Chemical and Biochemical Sciences, C. K. Tedam University of Technology and Applied Sciences, Navrongo, Ghana

<sup>2</sup> Department of Environmental Science, School of Environment and Life Sciences, C. K. Tedam University of Technology and Applied Sciences, Navrongo, Ghana



© The Author(s) 2023. **Open Access** This article is licensed under a Creative Commons Attribution 4.0 International License, which permits use, sharing, adaptation, distribution and reproduction in any medium or format, as long as you give appropriate credit to the original author(s) and the source, provide a link to the Creative Commons licence, and indicate if changes were made. The images or other third party material in this article are included in the article's Creative Commons licence, unless indicated otherwise in a credit line to the material. If material is not included in the article's Creative Commons licence and your intended use is not permitted by statutory regulation or exceeds the permitted use, you will need to obtain permission directly from the copyright holder. To view a copy of this licence, visit <http://creativecommons.org/licenses/by/4.0/>.

with high adsorption capacity. Hence, the adsorption behavior of CWFs should be very important to consumers due to the rise in chemical pollutants. CWFs are made with natural materials such as clay, rice husk, sawdust (Aliyu et al. 2019; Chaukura et al. 2020; Netti et al. 2019). The raw materials for the production of the filter are known adsorbents for their removal of cations and anions (Chai et al. 2020; Dan et al. 2021; Gu et al. 2019; Meez et al. 2021; Mohamed 2021; Nabieh et al. 2021; Otunola and Ololade 2020; Priya et al. 2022; Sanka et al. 2020). The adsorption capacity of clay has been widely reported with some clay materials having capacities as much as  $150 \text{ mgg}^{-1}$  (Chai et al. 2020; Kalebaila et al. 2018; Uddin 2017). Also, the adsorption potentials and capacity of biosorbents have been well documented (Madelá and Skuza 2021; Mohamed 2021; Naiya et al. 2009; Sanka et al. 2020). Studies have indicated the effectiveness of CWFs in the removal of microbes and suspended particles from raw water samples (Apea et al. 2023; Coleman et al. 2021; Ndebele et al. 2021; Shepard and Oyanedel-Craver 2022). Further, studies have equally found that the CWF materials exhibits adsorption potential as a result of their composition and their ability to exchange cations such as  $\text{Na}^+$ ,  $\text{Ca}^{2+}$  and  $\text{K}^+$ . Recent studies have highlighted the ability of the CWFs to remove charged ions from source water during filtration (Ajayi and Lamidi 2015; Bulta and Micheal 2019; Hussain and Al-Fatlawi 2020; Yang et al. 2020). However, there is no clear explanation of the adsorption behavior of the material. In contrast, some studies have questioned the viral and chemical correction ability of CWF materials (Ajayi and Lamidi 2015; Erhuanga et al. 2014). This indicates that there is a dearth of knowledge on the adsorption behavior of CWF materials.

Over the years, ceramists and material scientists have varied the source of clay samples and also modify the raw materials in the production of enhanced filter materials with high adsorption capacity (Abdullayev et al. 2019; Ajayi and Lamidi 2015; Akosile et al. 2020; Yang et al. 2020). This suggests that the trend of pollution in the world today where chemical pollutants (heavy metal ions) abound is of concern. Therefore, this study assesses the extent of Cu (II) ion's adsorption ability of pulverized samples of commercially available CWFs. In addition, the study compared the divalent metal ion adsorption behavior of the filter material during filtration to those of batch experiments.

## Materials and methods

### Sampling

The surface water sampling area is located in the Tamale township of the Northern Region of Ghana. The water sampling point was selected based on the characteristic,

composition and level of pollution. The sample was collected from the Dungu dugout with physicochemical characteristics as shown in Table 1. The water samples for filtration and assessment of divalent metal ion removability analysis of the CWFs were collected mid-stream at depths 20–30 cm directly into sterile 25 L PET gallons (Karikari and Ansa-Asare 2006). The water samples were conveyed to C.K. Tedom University of Technology and Applied Sciences chemistry laboratory, Navrongo and allowed to settle for a day before filtering with commercially available CWFs.

### Ceramic water filters (CWFs) sampling

Three types of ceramic water filters were purchased from the Ghanaian market. The filter materials were classified based on their shape, size and composition. The filters are ball filter (BF), hollow candle filter (CF) and pot filter (PF) as indicated in Fig. 1a–c respectively.

### Preparation of CWFs for batch adsorption experiments

The CWFs (BF, CF and PF) were separated into their components (Fig. 1a, b and c respectively) and pulverized with a mortar and pestle. The pulverized samples (CWFs) were sieved using different mesh sieves of sizes 100–500  $\mu\text{m}$  and stored in clean containers for the characterization and adsorption studies.

### Chemicals

All chemicals used in the study, including  $\text{CuSO}_4 \cdot 5\text{H}_2\text{O}$  (99.5% assay and 249.68 mg/mol), HCl (37% assay and 36.4 mg/mol), KCl (99.5% assay, 74.56 mg/mol and 1.19 specific gravity), and NaOH (99.5% assay, 40 mg/mol) were of analytical grade and purchased from Pan-reac Quimica, Spain. The  $\text{CuSO}_4 \cdot 5\text{H}_2\text{O}$  stock solution

**Table 1** Physicochemical parameters, dimensions and the composition of CWFs studied

Parameter	BF	BF with AC	CF	PF coated with colloidal silver
Flow rate (L/H)	$1.3 \pm 0.082$	$1.3 \pm 0.082$	$0.9 \pm 0.065$	$7.5 \pm 0.49$
pH (PZC)	$7.88 \pm 0.1$	$9.06 \pm 0.1$	$8.46 \pm 0.1$	$5.67 \pm 0.1$
pH	$7.88 \pm 0.1$	$9.06 \pm 0.1$	$8.45 \pm 0.1$	$5.69 \pm 0.1$
EC ( $\mu\text{S}/\text{cm}$ )	$724 \pm 11.2$	$1130 \pm 10.0$	$166 \pm 12.1$	$26 \pm 3.6$
Mass (g)	$182 \pm 3.4$	$230 \pm 2.5$	$310 \pm 1.8$	$3100 \pm 2.7$
App. porosity (%)	58.55	58.55	60.61	75.00
Height (cm)	$8.2 \pm 2.4$	$8.2 \pm 2.4$	$8.0 \pm 2.5$	$18.8 \pm 4.6$
Diameter (inner) cm	$8.9 \pm 3.3$	$8.9 \pm 3.3$	$5.3 \pm 2.0$	$34.7 \pm 4.3$
Diameter (outer) cm	$10.5 \pm 2.4$	$10.5 \pm 2.4$	$5.6 \pm 1.3$	$39.5 \pm 3.1$
Flow rate (L/H)	$1.3 \pm 0.082$	$1.3 \pm 0.082$	$0.9 \pm 0.065$	$7.5 \pm 0.49$

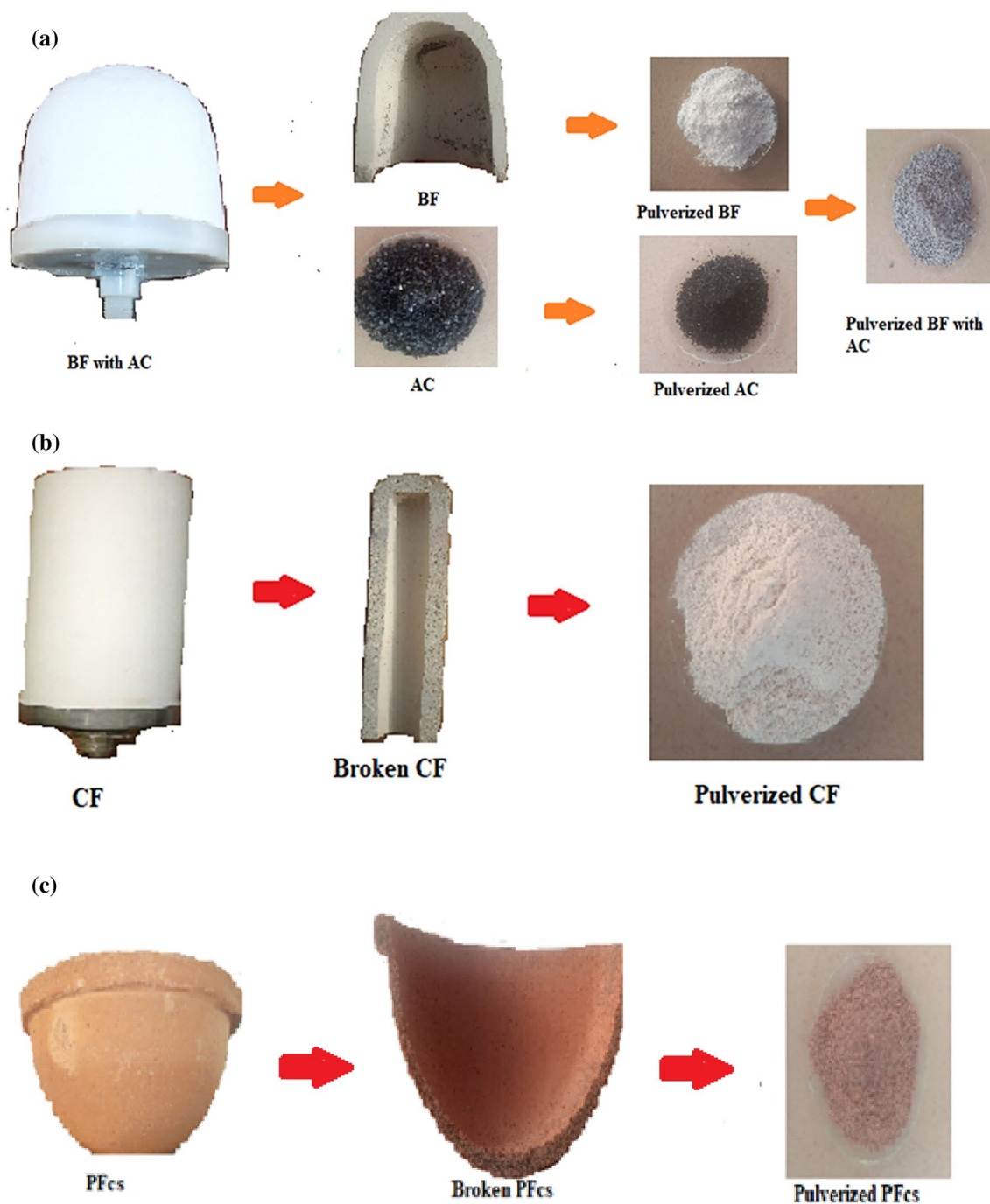


**Fig. 1** Samples of CWFs (a) BF, b CF and c PFcs used for the study

(1000 mg/L) was prepared by dissolving 3.2792 g  $\text{CuSO}_4 \cdot 5\text{H}_2\text{O}$  in distilled water (1000 mL). All solutions were freshly prepared by diluting the corresponding stock solutions with distilled water.

**Characterization of CWF materials**

The major oxide composition, functional groups, type of clay minerals, phases of the sintered CWF adsorbent and physicochemical properties of pulverized CWF

materials were characterized with a variety of analytical techniques. The major and minor oxides composition of the CWF materials, were analyzed with x-ray fluorescence spectrometer (XRF), (Venta VMR). The functional groups of the pulverized adsorbents were analyzed with Fourier-transform infrared spectrophotometer (FTIR), (Bruker-Vertex 60). The type of clay minerals and phase of the sintered CWF adsorbents were determined with x-ray powder diffractometer (XRD), (Panalytical Empyrean Series 2). The physicochemical properties such as the color of the CWFs, pH and EC of the pulverized CWF materials in deionized water, mass of the bulk filter and dimensions of the filter were determined.

#### **Determination of Point of Zero Charge**

The point of zero charge (PZC) is the pH at which the net charge on the particle's surface is equal to zero. This study determined the surface charge of the pulverized CWF materials with the aid of methods described by Bisaba (2015). A powdered sample of CWF (0.1 g) was weighed into 50 mL volumetric flask in replicates, followed by the addition of about 0.1 M HCl in specified volumes (5 mL, 10 mL, 15 mL, 20 mL, 25 mL, and 30 mL). Also, about 30 mL of distilled water was added 0.1 g of CWF materials to serve as a control. In addition, powdered sample of CWFs (0.1 g) was weighed into 50 mL volumetric flask in replicates, followed by the addition of about 0.1 M NaOH in specified volumes (5 mL, 10 mL, 15 mL, 20 mL, 25 mL, and 30 mL). the mixture was agitated with a mechanical shaker and allowed to stand for 48 h. The method was used for all powdered CWF (BF, CF, PE, AC and BF with AC) samples. The pH of the mixture was recorded after the duration and average pH was calculated for each volume of the mixture.

#### **Apparent porosity analysis of the CWF materials**

Apparent porosity of the commercially available CWF materials were determined using the water absorption test (direct) method, and the determination was repeated five times for each CWF as described in a study by Apea et al. (2023).. Apparent porosity (P) was then calculated using the expression stated in Eq. 1.

$$P(\%) = 100 \times \left( \frac{M_3 - M_1}{M_3 - M_2} \right) \quad (1)$$

where;  $M_3$  is the weight of the specimen when saturated in water;  $M_1$  is the weight of the dry specimen;  $M_2$  is the weight of the sample underwater.

#### **Chemical assessment of divalent metal ions uptake capacities of pulverized CWF materials**

##### **Determination of the effect of adsorbent dose**

To assess the effect of adsorbent dose on the extent of Cu (II) ions adsorption. About 20 mL of the copper solution

(100 mg/L) was added to 0.05 g of the pulverized adsorbent (AC). The mixture was agitated for ten minutes with a mechanical shaker at 100 rpm. At ten minutes, the interaction was terminated and the solid phase was separated from the solution using filtration method. The supernatant was then analyzed for its copper (II) ion content using a copper ion-selective electrode (ISE). The experiment was repeated independently for the AC adsorbent with varied masses of 0.10 g, 0.15 g, 0.20 g, 0.25 g, 0.30 g, 0.35 g and 0.40 g. Also, about 20 mL of the copper solution (100 mg/L) was added to 0.2 g of the pulverized CWF-adsorbent (BF, CF, PF and BF with AC). The mixture was agitated for ten minutes with a mechanical shaker at 100 rpm. At ten minutes, the interaction was terminated and the solid phase was separated from the solution using filtration method. The supernatant was then analyzed for its copper (II) ion content using a copper ion-selective electrode (ISE). The experiment was repeated independently for the AC adsorbent with varied masses of 0.4 g, 0.6 g, 0.8 g, 1.0 g and 1.2 g. All experiments were carried out in duplicates and the average values were used to estimate the equilibrium time.

##### **Determination of equilibrium time**

The effect of time on the adsorption of Cu (II) ions by CWF was determined. About 0.2 g of all CWFs and 0.05 g of AC were weighed into separate conical flasks. About 20 mL of the copper solution (1000 mg/L) was added and agitated with a mechanical shaker at 100 rpm for 30 min (for CF, BF and PFcs), 10 min (for BF with AC) and 5 min (for AC) as described by (Gupta et al. 2018) with slight modifications. The equilibrium time of copper (II) ions was measured by changing the time between the adsorbate (Cu(II) ions) and adsorbents (CWF) in the range of 30 to 300 min for CF, BF and PFcs, 10 to 120 min for BF with AC and 5 to 60 min for AC. All experiments were carried out in duplicates and the average values were used to estimate the equilibrium time.

##### **Determination of the effect of pH on adsorption**

The experiment for the effect of pH on the extent of Cu (II) ions adsorbed with CWF materials was conducted with 20 mL of Cu (II) ions solution (1000 mg/L) in a beaker containing 0.2 g of CWF material (powdered). To the mixture, 5 mL of the pH 2.0 buffer solution was added, followed by constant agitation for 120 min for PFcs, CF and BF, 40 min for AC and 90 min for BF with AC. The interaction was terminated by separating the solid phase (CWF material) from the solution phase using the filtration method. The supernatant was then analyzed for its copper (II) ion content using a copper ion-selective electrode (ISE). The experiment was repeated independently for pH values 3, 4, 5, 6, 7, and 8.

All experiments were carried out in duplicates. The procedure was repeated independently for 0.2 g of all CWFs and 0.05 g of activated carbon material (AC).

#### Determination of the effect of temperature on adsorption

About 0.2 g of CWF was added to a beaker containing 20 mL of Cu (II) ion solution (1000 mg/L). The temperature of the mixture was maintained at 20 °C with the adjustment of the temperature of water bath and agitated continuously for 120 min for PFCs, CF and BF, 40 min for AC and 90 min for BF with AC. The mixture was then filtered, and the supernatant was analyzed for Cu (II) ions with the aid of copper ISE. The experiment was repeated independently for 30, 40, 50, and 60 °C. In addition, all experiments were carried out in duplicates. The procedure was followed for 0.2 g of all other CWFs and 0.05 g of AC.

#### Determination of the effect of initial concentration on adsorption

About 0.2 g of CWF was added to a beaker containing 20 mL of Cu (II) ions solution (400 mg/L). The effect of the initial concentration was determined at a temperature of 27 °C and agitated continuously for 120 min for PFCs, CF and BF, 40 min for AC and 90 min for BF with AC. The mixture was then filtered, and the supernatant was analysed for Cu (II) ions with the aid of an Atomic Absorption Spectrophotometer (AAS). The experiment was repeated independently for 500, 600, 700, 800, 900 and 1000 mg/L. All experiments were carried out in duplicates. The procedure was followed for 0.2 g of all other CWFs and 0.05 g of AC.

The extent of adsorption by CWF-adsorbent ( $\text{mgg}^{-1}$ ) and percentage removal in the study was calculated using Eqs. (2) and (3).

$$\text{extent of adsorption, } q_e = \frac{(C_o - C_e)V}{m} \quad (2)$$

$$\% \text{ Removal} = \frac{C_o - C_e}{C_o} \times 100\% \quad (3)$$

where,  $C_o$  (mg/L)=Initial copper concentration of Cu (II) ions in aqueous solution,  $C_e$  (mg/L)=Equilibrium concentration of Cu (II) ions in aqueous solution,  $V$  (l)=Volume of Cu (II) ions sample taken and  $m$ =Mass of adsorbent taken.

#### Theoretical model

**Adsorption kinetics model** The equations of the pseudo-first-order (Demirbas et al. 2005) and the pseudo-second-order kinetic model (Edebali and Pehlivan 2014) were used to fit experiment data obtained from the batch

experiments. The formulas of the pseudo-first-order and the pseudo-second-order kinetic model are expressed as Eqs. (4) and (5), respectively.

$$\ln(q_e - q_t) = \ln q_e - k_1 t \quad (4)$$

$$\frac{t}{q_t} = \frac{1}{k_2 q_e^2} + \frac{1}{q_e} t \quad (5)$$

where  $q_t$  is the amount of Cu(II) ion adsorbed at time  $t$ ,  $\text{mg}\cdot\text{g}^{-1}$ ,  $k_1$  is the pseudo-first-order rate constant adsorption rate,  $\text{min}^{-1}$ ; and  $k_2$  is the adsorption rate constant in the pseudo-second-order kinetic rate constant,  $\text{g}\cdot\text{mg}^{-1}\cdot\text{min}^{-1}$ .

**Adsorption equilibrium** The isotherm models of Langmuir and Freundlich (Allwar et al. 2008) were tested to analyze the equilibrium data. The Langmuir isotherm model and Freundlich isotherm model equations are expressed by Eqs. (6) and (7).

$$\frac{C_{eq}}{q_e} = \frac{1}{q_{max}} C_{eq} + \frac{1}{q_{max} K_L} \quad (6)$$

$$\ln q_e = \ln K_f + \frac{1}{n} \ln C_{eq} \quad (7)$$

where  $q_{max}$  is the monolayer capacity of nano I-S<sub>m</sub>,  $\text{mg}\cdot\text{g}^{-1}$ ;  $K_L$  is the Langmuir constant,  $\text{L}\cdot\text{mg}^{-1}$ ;  $K_f$  is the Freundlich constant,  $\mu\text{g}\cdot\text{g}^{-1}$ ; and  $n$  is the heterogeneity.

#### Adsorption thermodynamics

The thermodynamic parameters can be determined using the equilibrium constant and temperature (Saha and Chowdhury 2011). The change in the Gibbs free energy ( $\Delta G$ ), enthalpy ( $\Delta H$ ), and entropy ( $\Delta S$ ) in the adsorption process was calculated using Eqs. (8) and (9).

$$\Delta G = -RT \ln K_d \quad (8)$$

$$\ln K_d = \frac{\Delta S}{R} - \frac{\Delta H}{RT} \quad (9)$$

where  $R$  is the universal gas constant,  $8.314 \text{ J}\cdot\text{mol}^{-1}\cdot\text{K}^{-1}$ ;  $T$  is the absolute temperature, K; and  $K_d$  is the distribution coefficient of metal ions I-S<sub>m</sub>,  $K_d = q_e / C_{eq}$ .

#### Filtration experiment

The surface water filtration with commercially available CWFs was conducted as indicated in the setup in Fig. 2. Initially, the CWFs were thoroughly washed with distilled water which was in line with the guidelines of manufacturers before use. This is done to avoid possible leachates.

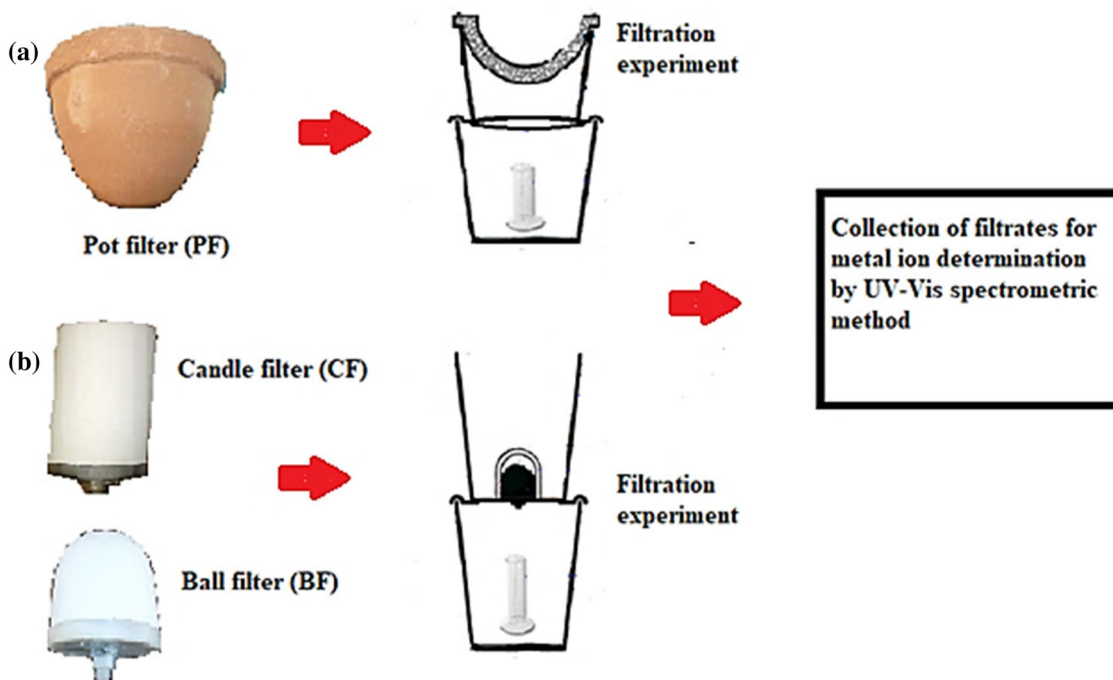


**Fig. 2** Schematic diagram of setup for filtration experiments: Setup for **a** pot filter and **b** candle or ball filter

The filter materials were soaked in the distilled water overnight. Then the distilled water was allowed to percolate the filter until the filtrate were clear. The filters (BF, CF and PF) were fitted in a container and raised above a receptacle containing a measuring cylinder (Fig. 2). The surface water was allowed to percolate the CWFs into the measuring cylinder while samples were collected simultaneously at thirty minutes (30 min) intervals for divalent metal ions (Fe (II) and Mn (II) ions) analysis. The flow rate of the CWFs was determined using the relation in Eq. 10.

$$\text{Flow Rate(L/H)} = \frac{\text{Volume of water (L)}}{\text{(time taken (H))}} \tag{10}$$

**Result and discussion**

**Characterization**

The commercially available CWFs were characterized in terms of their mass, height, color, pH, electrical conductivity and the composition of the major oxides, functional groups, type of clay minerals and phase. Table 1 presents information on the mass, dimensions, flow rate, pH and electrical conductivity of the CWFs.

**Characterization of pulverized CWF materials**

Table 1 shows that the pH of the pulverized commercially available CWF materials are 5.67, 7.88, 8.46 and 9.06 for PFcs, BE, CF and BF with AC, respectively.

The observed pH does not vary from the pH of the point of zero charge (PZC) which implies that the charge on the surfaces of the filter materials does not change in water. The pH (PZC) of the CWFs was 5.67 (PFcs), 7.88 (BF), 8.46 (CF), 8.45 (AC) and 9.06 (BF with AC) as observed in Table 1. This indicates that when the pulverized CWF materials are kept in a solution with a pH less than that of the pH of the PZCs, the surface of the materials will be more positively charged and could attract negatively charged ions (anions) and vice versa. The study purposively assessed the PZC of the filter materials because it is one of the factors that suggest the ability of the filter material to adsorb ions and the type of ions (anions or cations) that could be adsorbed at specified pH values. It could be inferred from the pH (PZC) that the pulverized CWF materials (BE, CF, AC and BF with AC) could attract cations but not as much as PF in water when pH ranges from 6–7. The materials showed electrical conductivity (EC) in deionized water as follows; BF with AC (1130 μS/cm), BF (724 μS/cm), CF (166 μS/cm) and PF (26 μS/cm) suggesting that BF with AC has more ions in solution. The mass (gram) of the bulk filter materials were PF (3100), CF (310), BF with AC (230) and BF (182) which indicates that PF is heavier than all commercially available CWFs. The apparent porosity of the filter materials was 58.55%, 60.61% and 75.00% for BF with AC, CF and PF respectively. The porosity of the filter material indicates that PF has the highest apparent porosity. It

could be inferred from Table 1 that the apparent porosity of the CWFs increases as the mass of the materials increase. In addition, the mass of CWFs varies in the order: PFcs > CF > BF with AC. The dimensions of CWFs indicate that PFcs are large but BF and CF are small and potable. The flow rate of the CWFs were 0.9 L/H (CF), 1.3 L/H (BF and BF with AC) and 7.5 L/H (PFcs).

The elemental composition of CWFs is provided in Table 2 as evaluated by X-ray fluorescence.

The major elements in all the CWFs are silica (SiO<sub>2</sub>) and alumina (Al<sub>2</sub>O<sub>3</sub>) followed by Fe<sub>2</sub>O<sub>3</sub>, K<sub>2</sub>O and CaO which are present in moderate concentrations (mg/L0.075–10.69%). The rest of the oxides are present in small quantities (0.0079–1.29%)mg/L). The concentration of CaO is well known (Bonis et al. 2017) to decrease the red color of iron in clay material and this may explain the observed white to the off-white color of BF with AC and CF (CWFs). The quantity of alumina and silica are 10.14% and 45.34% for PFcs, 7.18% and 44.62% for BF with AC and 20.73% and 47.34% for CF (Table 2). The red color of PFcs could be attributed to the use of iron-rich clay for its production. The loss on ignition value indicates that the CWFs (PFcs, BF with AC and CF) has higher carbonaceous matter (as the result of the addition of the burn out material before firing) and relatively high content of mineral contents.

The possible minerals with their 'd' values of PFcs, BF, BF with AC, CF and AC are presented in Fig. 3a–e respectively. Both the quantitative and qualitative phases in the CWF-adsorbents have been made but their characterization of XRD patterns indicates the presence of quartz, carbon, graphite, muscovite and wollastonite as

the major phases. The PFcs adsorbent is made up of 49.6 percent of quartz (SiO<sub>2</sub>) and 50.4 percent of muscovite (KAl<sub>2</sub>(Si<sub>3</sub>Al)O<sub>10</sub>(OH)<sub>2</sub>) as indicated in Fig. 3a. Also, the BF adsorbent is made up of 72.2% of quartz and 27.8% of wollastonite (CaSiO<sub>3</sub>) as indicated in Fig. 3b. In addition, the combination of the BF with AC adsorbent with the percentage ratio of 72.7 to 27.3 respectively indicates the presence of 2.5% of carbon, 50.7% of graphite, 35.1% of quartz and 11.7% of wollastonite as indicated in Fig. 3c. Also, the CF adsorbent is made up of 92.1% of quartz and 7.7% of wollastonite as indicated in Fig. 3d. the study revealed that the XRD of the activated carbon in the BF contain 8.6% of carbon and 91.4 percent of graphite as indicated in Fig. 3e. Further, the occurrence of the above minerals, the CWF-adsorbents was confirmed by FTIR study to assessed the possible minerals present. **Fig. 3** Powder XRD patterns of **a** PFcs, **b** BF, **c** BF with AC, **d** CF and **e** AC

However, all CWF-adsorbents were sintered at 800 to 950 °C, this could contribute to the non-existence of O–H group around the 3000 range as observed in Fig. 4a–e. This observation corroborates with study by Nawang et al. (2019). The results of PFcs (Fig. 4a) suggest that the possible minerals present are feldspar (1023.47 cm<sup>-1</sup>, splitting bands in the region 800 -400 cm<sup>-1</sup> including 777.92 cm<sup>-1</sup>). The spectra of the PFcs adsorbent confirmed the presence of the muscovite (777.92 cm<sup>-1</sup> and 1023.47 cm<sup>-1</sup>) and quartz (1991.23 cm<sup>-1</sup>, 1963.88 cm<sup>-1</sup>, 1023.47 cm<sup>-1</sup> and 777.92 cm<sup>-1</sup>) as indicated by the XRD result in Fig. 3a. The results of BF (Fig. 4b) suggest that the possible minerals present are feldspar (1011.32 cm<sup>-1</sup>, splitting bands in the region 800 -400 cm<sup>-1</sup> including 793.55 cm<sup>-1</sup> and 446.23 cm<sup>-1</sup>), hematite (689.07 cm<sup>-1</sup> and 565.95 cm<sup>-1</sup>), anhydrite (936.72 cm<sup>-1</sup> and 565.95 cm<sup>-1</sup>), traces of kaolinite (1011.32 cm<sup>-1</sup>, 689.07 cm<sup>-1</sup> and 446.23 cm<sup>-1</sup>) and traces of carbonates (1981.16 cm<sup>-1</sup>, 900.07 cm<sup>-1</sup> and 731.12 cm<sup>-1</sup>). The spectra of the BF adsorbent confirmed the presence of the wollastonite (900.07, 936.72 and 1011.32) and quartz (1981.16 cm<sup>-1</sup>, 1011.32 cm<sup>-1</sup>, 776.20 cm<sup>-1</sup>, 731.12 cm<sup>-1</sup>, 689.09 cm<sup>-1</sup>, 565.93 cm<sup>-1</sup> and 446.23 cm<sup>-1</sup>) as indicated by the XRD result in Fig. 3b. The results of BF with AC (Fig. 4c) suggest that the possible minerals present are feldspar (1010.84 cm<sup>-1</sup>, splitting bands in the region 800 -400 cm<sup>-1</sup> including 776.35 cm<sup>-1</sup>, 683.34 cm<sup>-1</sup> and 454.05 cm<sup>-1</sup>), hematite (683.34 cm<sup>-1</sup> and 567.23 cm<sup>-1</sup>), magnesium-rich chlorite (1981.16 cm<sup>-1</sup>, 1010.84 cm<sup>-1</sup>, 899.32 cm<sup>-1</sup>, 683.34 cm<sup>-1</sup>, 645.98 cm<sup>-1</sup> and 567.23 cm<sup>-1</sup>), traces of kaolinite (1010.84 cm<sup>-1</sup>, 683.34 cm<sup>-1</sup> and 454.05 cm<sup>-1</sup>) and traces of carbonates (1970.88 cm<sup>-1</sup>, 899.32 cm<sup>-1</sup> and 726.02 cm<sup>-1</sup>). The spectra of the BF with AC adsorbent confirmed the presence of the wollastonite (899.32 cm<sup>-1</sup>, 836.42 cm<sup>-1</sup> and 1010.84 cm<sup>-1</sup>) and quartz (1970.88 cm<sup>-1</sup>, 1010.84 cm<sup>-1</sup>, 776.35 cm<sup>-1</sup>, 731.12 cm<sup>-1</sup>,

**Table 2** Chemical composition of Commercially Available Ceramic Water Filters (CWFs) (%)

Compounds	wtt (%) present in Commercially Available CWF-Adsorbents				
	PFcs	BF	AC	CF	BFwith AC
SiO <sub>2</sub>	45.34	55.24	3.55	47.34	44.62
Al <sub>2</sub> O <sub>3</sub>	10.14	8.46	1.18	20.73	7.18
Fe <sub>2</sub> O <sub>3</sub>	5.13	0.48	0.39	1.12	0.39
CaO	0.075	10.69	1.63	3.23	8.54
K <sub>2</sub> O	2.57	3.28	0.82	0.46	2.64
TiO <sub>2</sub>	0.74	n.d	n.d	1.29	n.d
MnO	0.031	0.020	0.0079	0.0085	0.015
MgO	n.d	n.d	1.82	n.d	n.d
I.L	35.55	21.62	89.67	25.62	36.41
SiO <sub>2</sub> /Al <sub>2</sub> O <sub>3</sub> molar ratio	~ 4	~ 6	~ 3	~ 2	~ 5

NB: n.d not detectable

Ignition Loss (I.L) is determined by burning one gram sample at 1000 °C till constant weight

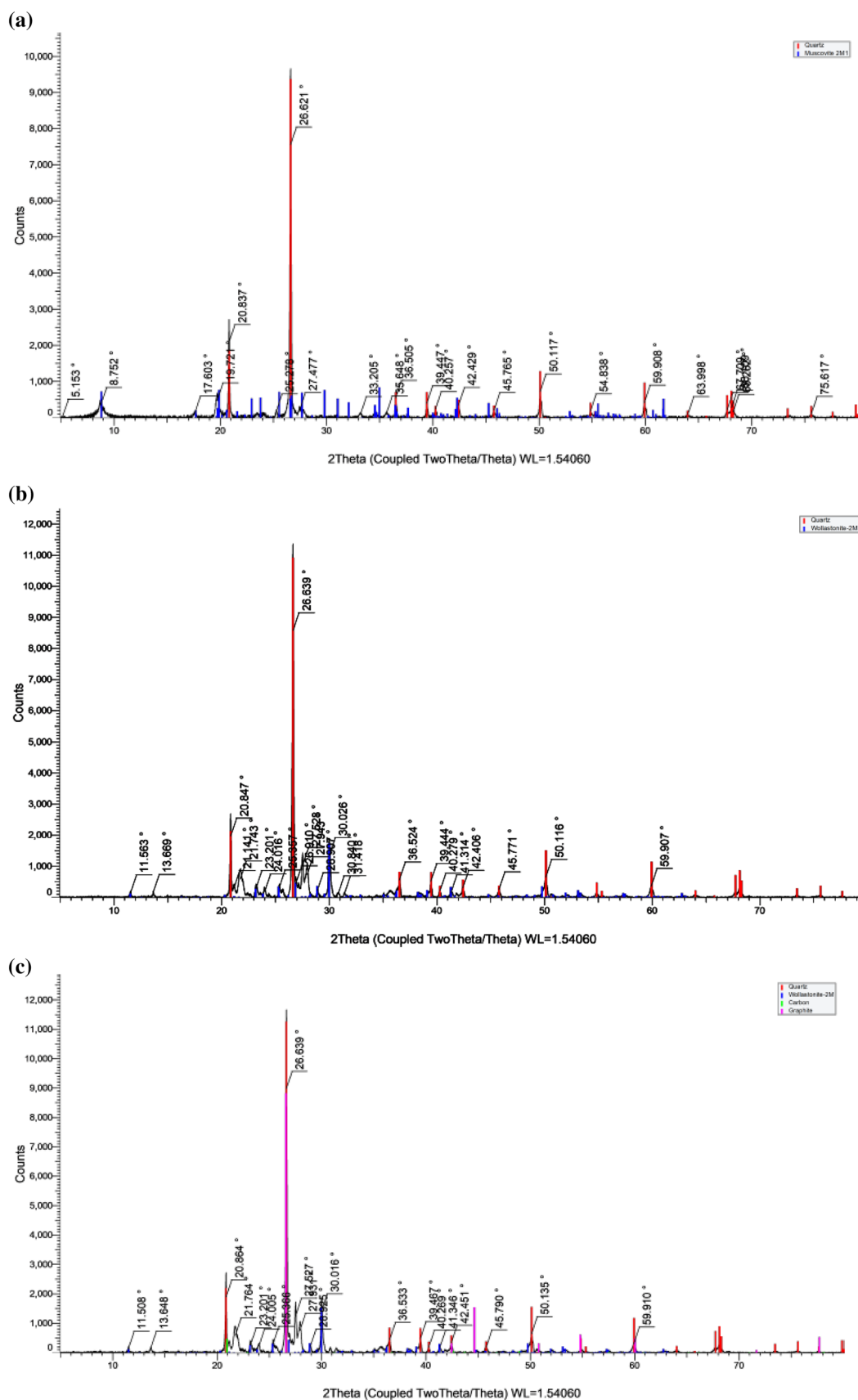


**Fig. 3** Powder XRD patterns of **a** PFcs, **b** BF, **c** BF with AC, **d** CF and **e** AC

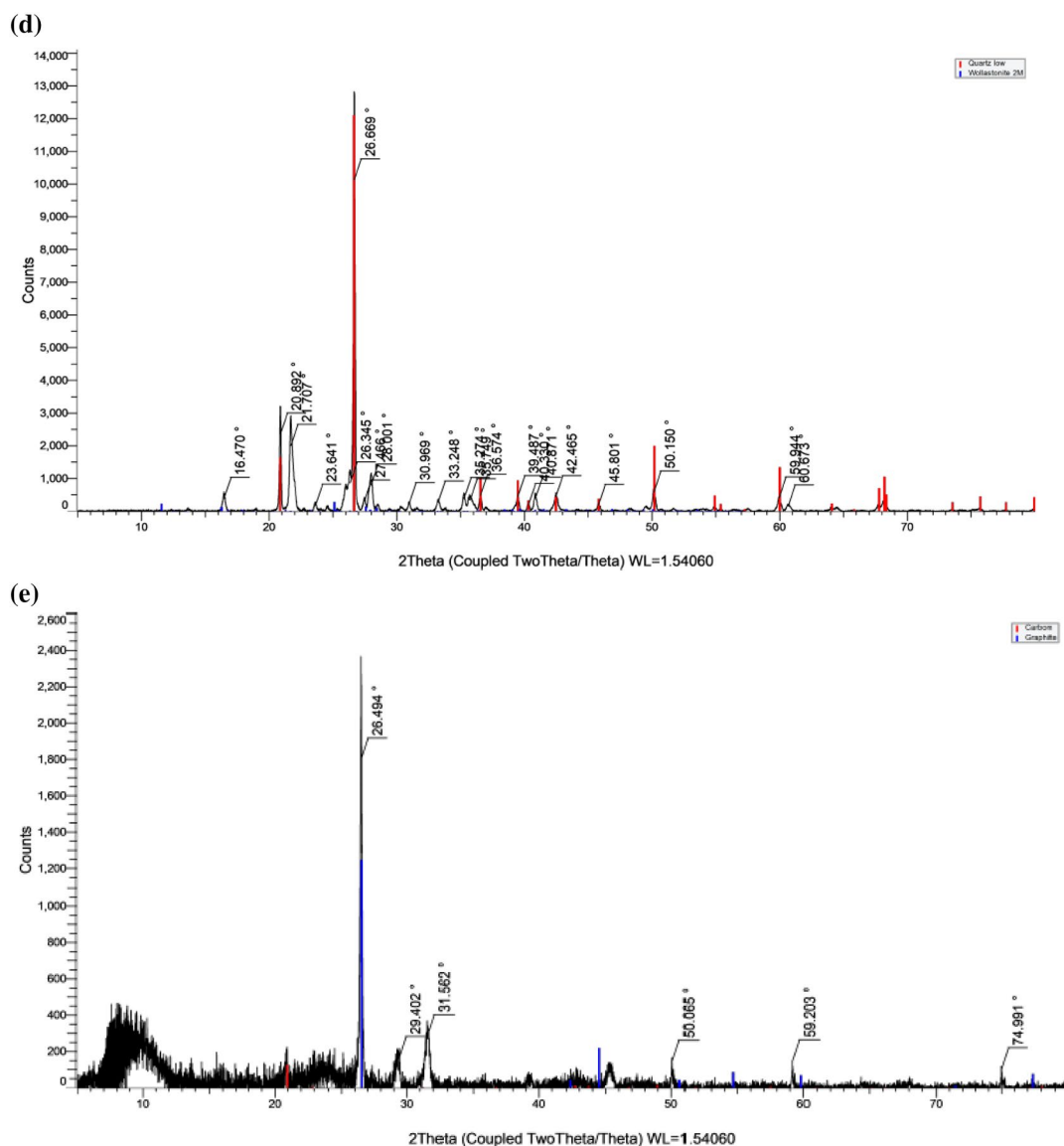


Fig. 3 continued

683.34  $\text{cm}^{-1}$ , 567.23  $\text{cm}^{-1}$  and 454.05  $\text{cm}^{-1}$ ) as indicated by the XRD result in Fig. 3c. The results of CF (Fig. 4d) suggest that the possible minerals present are feldspar (1079.05, splitting bands in the region 800–400  $\text{cm}^{-1}$  including 776.49  $\text{cm}^{-1}$  and 539.26  $\text{cm}^{-1}$ ), hematite (908.93  $\text{cm}^{-1}$ ), smectite (3852.76  $\text{cm}^{-1}$ , 1079.05  $\text{cm}^{-1}$ , 908.93  $\text{cm}^{-1}$  and 539.26  $\text{cm}^{-1}$ ), traces of illite (3852.76  $\text{cm}^{-1}$ , 1079.05  $\text{cm}^{-1}$  and 539.26  $\text{cm}^{-1}$ ), anhydrite (908.93  $\text{cm}^{-1}$  and 539.26  $\text{cm}^{-1}$ ) and traces of carbonates (1984.95  $\text{cm}^{-1}$ , 908.93  $\text{cm}^{-1}$  and 776.49  $\text{cm}^{-1}$ ). The spectra of the CF adsorbent confirmed the presence of the wollastonite (908.93  $\text{cm}^{-1}$  and 1079.05  $\text{cm}^{-1}$ ) and quartz (1984.95  $\text{cm}^{-1}$ , 1079.05  $\text{cm}^{-1}$ , 776.49  $\text{cm}^{-1}$  and 539.26  $\text{cm}^{-1}$ ) as indicated by the XRD result in Fig. 3d.

The above minerals suggested are in line with a study conducted by Nayak and Singh (2007). In addition, all CWF-adsorbent (especially, AC of Fig. 3e) showed C-H bond from 1923,27 to 1991.86  $\text{cm}^{-1}$  and O=C=O group found from 2000 to 2500  $\text{cm}^{-1}$ . **Fig. 4** FTIR patterns of **a** PFcs, **b** BF, **c** BF with AC, **d** CF and **e** AC

#### Characteristics of raw water

The characteristics of the raw water (Table 3) indicate that the general characteristics of the Dungu dugout water sample fall out of the acceptable limit recommended by WHO (2011), with turbidity (1800 NTU),

concentration of iron (6.50 mg/L), concentration of manganese (1.962 mg/L) and total coliform (178 cfu/mL).

These parameters were higher than the maximum acceptable limits recommended by WHO (2011). The metal ion concentration of the raw water justifies the treatment with the commercially available CWFs. After filtration with the commercially available CWFs, the physicochemical characteristics of the filtrates are presented in Table 4. The average values of parameters (E.C, pH and total hardness) of the filtrate of the CWFs are higher than that of the raw water sample. The elevation of the values of the parameters could be as a result of adsorption/desorption of charged species as suggested in a study by Apea et al., (2023). Although the values of the above-mentioned parameters are relatively higher compared to that of the raw water sample, yet the values conform with that of the WHO/GWCL standards.

The average concentration of divalent ions of the filtrate of CWFs are presented in Table 4. The result indicates that CWFs are efficient in divalent metal ions ( $\text{Fe}^{2+}$  and  $\text{Mn}^{2+}$ ) removal (sorption). As shown in Table 3 concentration (mg/L) of  $\text{Fe}^{2+}$  of the raw water sample was 6.50. However, PFcs reduced the concentration to 3.33 mg/L, CF also reduce the concentration to 1.70 mg/L and BF with AC reduced the concentration to 0.19 mg/L. In addition, the concentration of  $\text{Mn}^{2+}$  as indicated as 1.982 mg/L of the raw water sample was reduced after filtration by the CWFs (PFcs, CF and BF with AC) to 0.911 mg/L, 0.795 mg/L and 0.025 mg/L respectively. The concentration of divalent metal ions of filtrates of PFcs and CF were out of the specifications of the WHO/GWCL standards. The order of divalent sorption efficiency during filtration is BF with AC > CF > PFcs.

#### Adsorption behavior of pulverized commercially available CWFs

##### *The effect of adsorbent dose*

The effect of the mass of adsorbent on copper uptake capacity ( $q_e$ ) was found to reduce with an increase in quantity of the adsorbent (CWF), this could be a result of the fact that the system was at equilibrium (Fig. 5a–e). The observation corroborated a study by (Fahmi et al. 2011), which indicates that the removal rate of an adsorbent does not increase with the continuous increase of the adsorbent dose. The decreased copper uptake value (mg Cu/g of CWF material) is due to the splitting effect of the flux (concentration gradient) between the CWF and Cu (II) ions (Nandi et al. 2008). This implies that the addition of more adsorbent reduces the adsorption efficiency of the adsorbent per unit mass. Therefore, the maximum adsorption was noted at 0.05 g (AC) and 0.2 g (BF with AC, PFcs, BF and CF) adsorbent masses. Thus, 0.05 g and 0.2 g were chosen as the maximum adsorbent

dose. The equilibrium time experiment selected for the study was 120 min for PFcs, CF and BF, 40 min for AC and 90 min for BF + AC.

##### *The kinetic behavior of Cu (II) sorption by selected CWFs*

The correlation coefficients ( $R^2$ ) are nearer to 1 for pseudo-second-order kinetics compared to pseudo-first-order as indicated in Table 5. This implies that the pseudo-second-order model can better describe the adsorption process. This suggests that Cu (II) ions sorption by CWF-adsorbent could be chemisorption. The copper(II) ions stick to the surface of CWF material hence forming a chemical compound (usually covalent) bond and tend to locate available binding sites that maximize their coordination number with the adsorbent surface (Atkins 1995).

The pseudo-second-order kinetic analysis reveals that the values of the initial adsorption rates ( $h$ ) increase with an increase in the initial copper concentration in the order: AC > BF with AC > PF > BF > CF, but the rate constant ( $k$ ) decreases with an increase in initial copper concentration (Table 5). This is as a result of the lower competition for the available binding sites at low concentrations. At higher concentrations, the competition for the available binding sites is high and consequently, lower sorption rates could be obtained (Wong et al. 2003). The extent of adsorption at equilibrium ( $q_e$ ), however, increases by increasing the initial copper concentration of copper ions and the ions could be adsorbed at the available binding sites. Comparing the calculated amount adsorbed  $q_e$  (mgg<sup>-1</sup>), CWFs (BF, PFcs and CF) sorption capacities were in the order of PF > BF > CF. But the amount of Cu (II) ion adsorbed by AC was greater and this could be attributed to the pre-treatment of the composite (AC). When the composite was added to BF (i.e., BF with AC), it was observed that the extent of sorption of the BF with AC increased by 85.7%. This suggests that AC improved the extent of sorption of CWF materials. The kinetic behavior of all CWFs suggested that the mechanism of the adsorption process could be chemisorption.

##### *The effect of initial pH on copper (II) ion uptake by CWFs*

The results as observed in Fig. 6 indicates that the percentage of the extent of adsorption of Cu (II) ions for AC increased from 59.5 to 96.7% for a rise in pH value from 2 to 7 and also 64.4 to 97.3% for an increase in pH value from 2 to 8 for BF, BF with AC, PFcs and CF.

Further increase in pH of the solution (pH 8), resulted in desorption for all CWF adsorbents. The main composition of the filter materials (clay and combustible material (activated carbon)) is known for their negative surface charges in solution at high pH depending on the

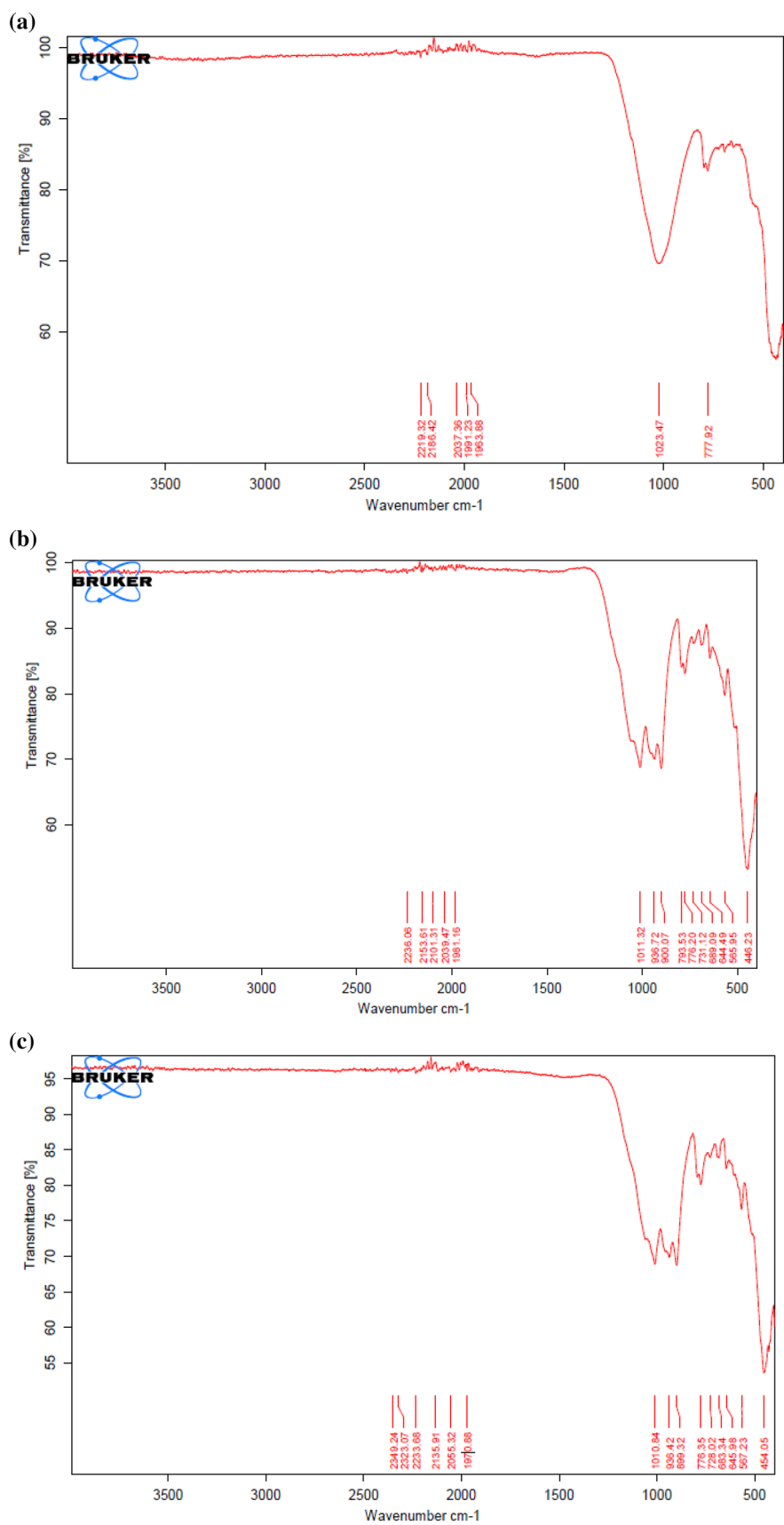


**Fig. 4** FTIR patterns of **a** PFcs, **b** BF, **c** BF with AC, **d** CF and **e** AC

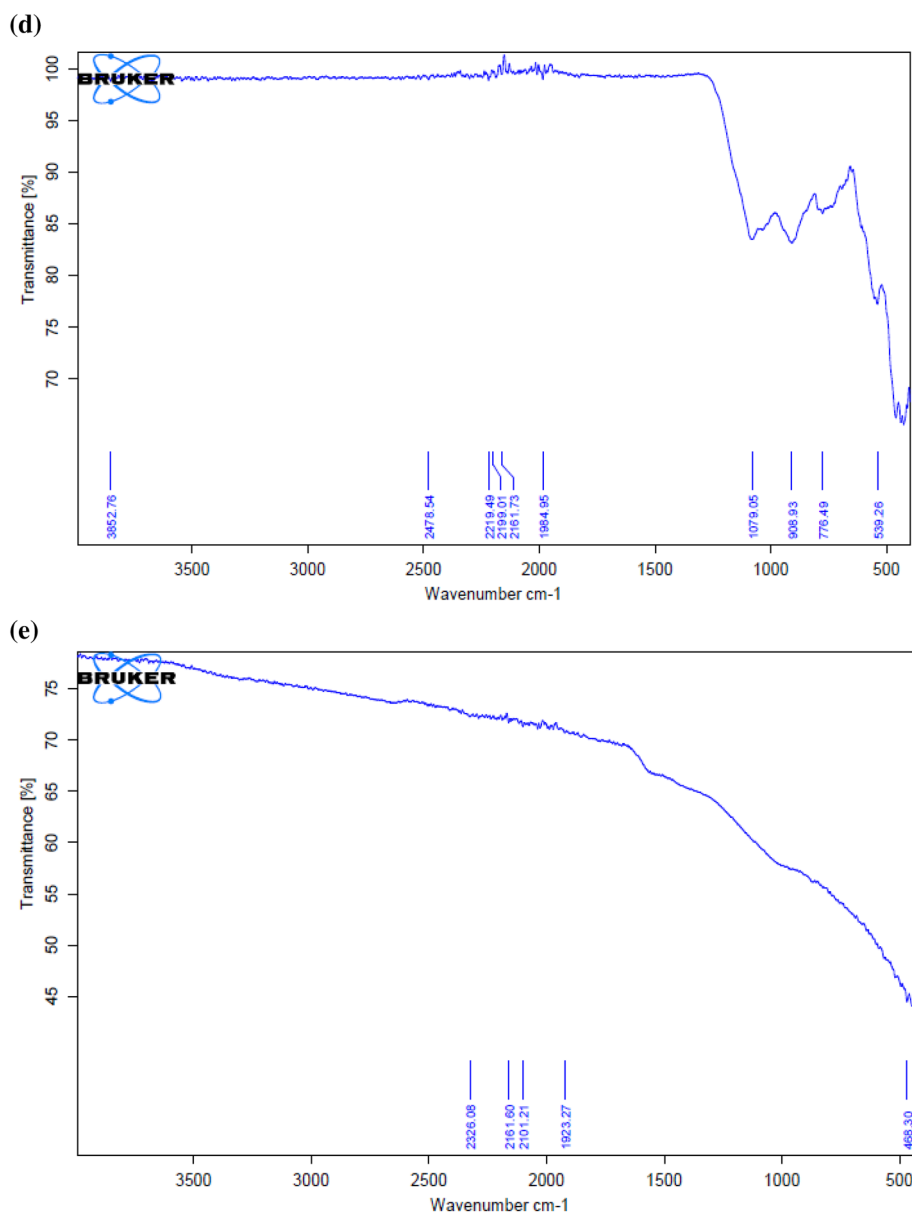


Fig. 4 continued

**Table 3** Physicochemical characteristics of raw surface water

Parameter	Sample Dungu dam	WHO standard
Turbidity (NTU)	1800 ± 26.46	5
E.C. (µS/cm)	179.6 ± 3.61	1000
TDS (mg/l)	89.8 ± 4.55	1000
Fe (mg/l)	6.50 ± 0.04	0.3
Mn (mg/l)	1.982 ± 0.05	0.4
Total Hardness (mg/l)	16 ± 2.08	300
pH	6.66 ± 0.55	6.5–8.5
T. Col. (cfu/ml)	178 ± 1	0

NB n.d = not detectable

pzc (Ismadji et al. 2015; Momina and Isamil 2018). As pH values change, the charge on the surface of the material also changes, hence the adsorption of charged species.

Also, it is likely that at low pH values, where there are more H<sup>+</sup>/H<sub>3</sub>O<sup>+</sup> ions in solution, competition occurs between the positively charged H<sup>+</sup> species and the metal ions for the existing binding sites on the negatively charged surface of the CWF materials. In a case where pH rises to 7 and the balance between H<sup>+</sup>/H<sub>3</sub>O<sup>+</sup> and OH<sup>-</sup> are equal, more of the Cu (II) ions in solution were taken, by the extent limit on the negative CWFs surface. Therefore, the percentage of the Cu (II) ions adsorbed raised, this is observed for all CWF materials

**Table 4** Physicochemical characteristics of Filtrates of CWF materials

Parameter	Filtrates of CWFs			WHO standard
	PFcs	BF with AC	CF	
E.C. ( $\mu\text{S}/\text{cm}$ )	192.1 $\pm$ 2.51	437.0 $\pm$ 2.70	421.0 $\pm$ 3.61	1000
pH	7.36 $\pm$ 0.10	7.54 $\pm$ 0.075	7.65 $\pm$ 0.10	6.5–8.5
Total Hardness (mg/l)	29.0 $\pm$ 1.61	27.0 $\pm$ 1.73	36.0 $\pm$ 1.73	300
Fe (mg/l)	3.33 $\pm$ 0.058	1.70 $\pm$ 0.040	0.19 $\pm$ 0.040	0.3
Mn (mg/l)	0.911 $\pm$ 0.001	0.795 $\pm$ 0.001	0.025 $\pm$ 0.001	0.4

at a pH of 7. On the other hand, in the alkaline range, it is assumed that precipitation of  $\text{Cu}(\text{OH})_2$  could occur, which may lead to a consistent decrease in Cu (II) ions but not necessarily been adsorbed by CWF materials. However, at low copper concentrations, Cu (II) ions are the main species at low pH values up to pH 7.5 and at high pH values,  $\text{Cu}(\text{OH})_2$  is the main species up to pH 12.3 (Albrecht et al. 2011). This indicates that the optimum sorption of copper ions by CWFs occurred at pH 7.0. It could be conclusive that the amount recorded for adsorption in this study is solely interaction between copper ions and CWF materials since  $\text{Cu}(\text{OH})_2$  is formed at  $\text{pH} > 7.5$ . This implies that for the pH of potable water which ranges from 6.5 to 8.5 (WHO/GWCL standard), When water samples are within the pH range, maximum metal removability will occur at pH of 7 and beyond pH of 7.5 some of the metals could change chemical form and leach into the filtrate of CWFs.

#### Effect of temperature on the sorption behavior of selected CWF materials

The copper (II) ions uptake by CWFs was studied as a function of temperature which revealed that the maximum adsorption occurred at 343 K as shown in Fig. 7.

It is observed from Fig. 7 that there was a gradual rise in Cu (II) ions adsorbed by CWF materials as temperature increases from 273 to 343 K. The adsorption increased with increasing temperature with a slight decrease at 320 K for all CWFs, suggesting that the process is endothermic. Therefore, higher temperatures might have facilitated the adsorption of Cu (II) ions by the CWF materials. It implies that with high temperatures during filtration, metal ions could be removed by the CWFs. Although the filters adsorb Cu (II) ions at high temperatures, at room temperature, 298.15 K, the CWFs also have the capacity to adsorb metal ions.

#### The activation energy ( $E_a$ )

The activation energy of the CWF materials,  $E_a$  is defined as the energy that must be overcome by Cu (II) ions to interact with the functional groups on the surface of the

CWFs. As indicated in Table 6, it is observed that values of  $E_a$  are in the range of +19.30 to +25.21 kJ/mol, which indicates that the values fall in the range of +8.4 to +83.7 kJ/mol (Saha and Chowdhury 2011), this implies, the sorption of copper ion onto CWF materials could be a chemisorption process. Also, it conforms to chemisorption compound formation since this process requires high activation energy. Moreover, the amount of energy required for the activation complex to be achieved for the adsorption of Cu (II) ions to occur is less than the amount of energy given to the system. This suggests that the process is favorable and feasible.

#### Free energy ( $\Delta G^\circ$ ), enthalpy ( $\Delta H^\circ$ ) and entropy ( $\Delta S^\circ$ )

The sorption of copper on CWF materials increased from 283 to 343 K (Fig. 7). The adsorption process was endothermic. The values of the enthalpy ( $\Delta H^\circ$ ) and entropy ( $\Delta S^\circ$ ) changes were found to be +48.21 kJ/mol and +0.433 kJ/Kmol for AC, +114.22 kJ/mol and +0.574 kJ/Kmol for BF with AC, +115.65 kJ/mol and +0.576 kJ/Kmol for BF, +101.55 kJ/mol and +0.532 kJ/Kmol for PFcs and +91.43 kJ/mol and +0.502 kJ/Kmol for CF respectively as indicated in Table 6. The positive values of the  $\Delta H^\circ$  confirm the endothermic nature of the sorption and the value of  $\Delta S^\circ$  indicate the change in the randomness of the CWF adsorbent-solution interface during sorption. Furthermore, the  $\Delta H^\circ$  values of the sorption between the CWF materials and Cu (II) ions are greater than 40 kJ/mol but less than 240 kJ/mol which suggests that the process is chemisorption.

The negative values of  $\Delta G^\circ$  indicate that the process is feasible and the sorption process is spontaneous. From Table 6 the  $\Delta G^\circ$  values ranged from -47.452 to -100.214. The  $\Delta G^\circ$  values up to -20 kJ/mol are consistent with electrostatic interactions between adsorbed site and the charged ions (physisorption), while  $\Delta G^\circ$  values negative and larger than -40 kJ/mol involved charge distribution or transfer from the biomass surface to the charged ions to form a coordinate covalent bond (chemisorption) (Horsfall et al. 2004; Kumar et al. 2010). The  $\Delta G^\circ$  values

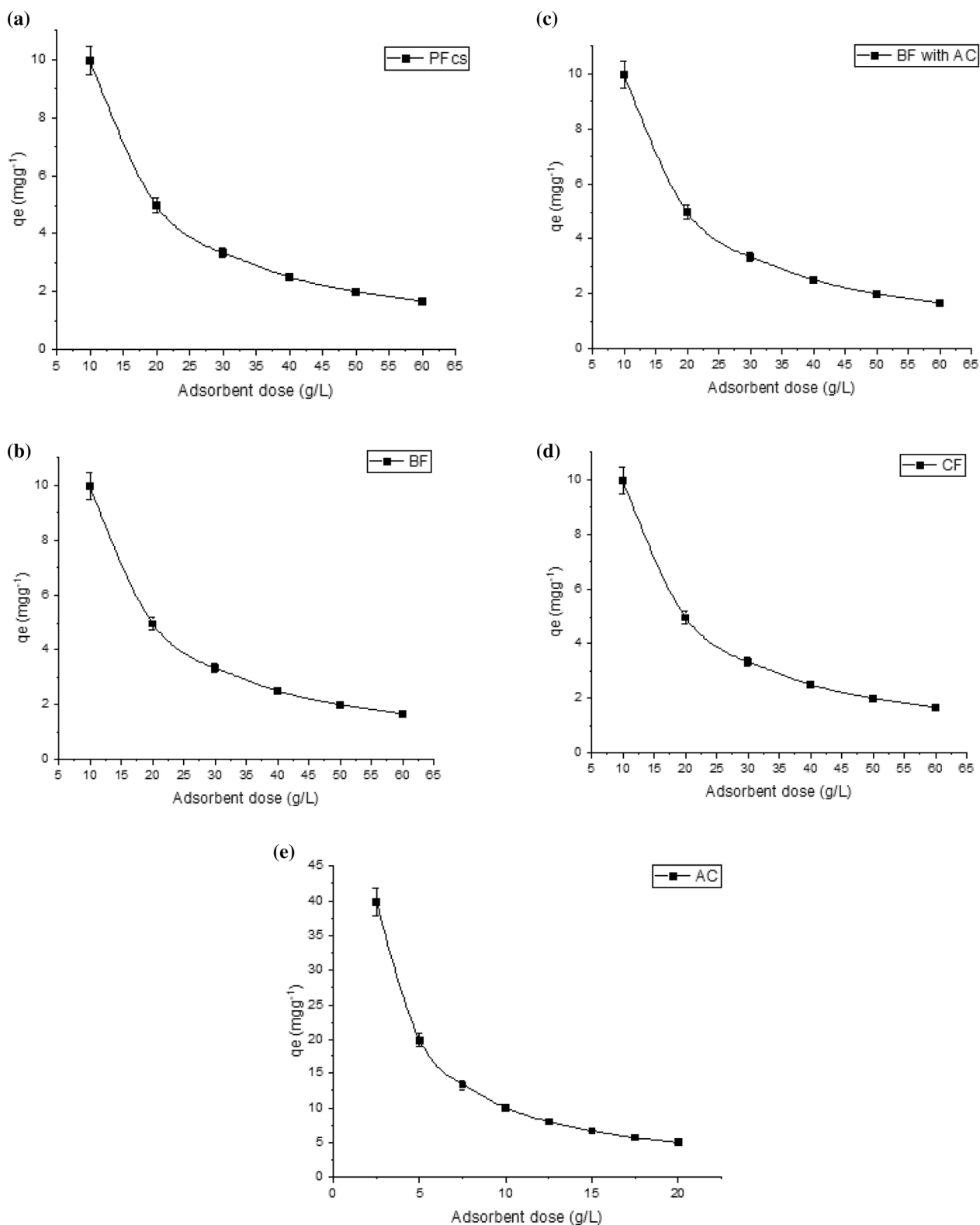


**Fig. 5** The extent of Cu (II) ions adsorbed by **a** PFcs-adsorbent, **b** BF-adsorbent, **c** BF with AC-adsorbent, **d** CF-adsorbent and **e** AC adsorbent against adsorbent dose

**Table 5** Kinetic model parameters of the compositions of selected CWFs

Kinetic models		CWF				
		AC	BFwithAC	BF	PFcs	CF
Pseudo first order	$k_1(\text{min}^{-1})$	0.015660	0.001382	0.002994	0.000691	0.000092
	$q_e(\text{mg/g})$	0.416100	0.858000	0.530000	1.040000	0.896000
	$R^2$	0.785200	0.323000	0.408600	0.217600	0.011100
Pseudo second order	$k_2(\text{mgg}^{-1} \text{min}^{-1})$	0.000170	0.003168	0.002207	0.004489	-0.097288
	$h(\text{mgg}^{-1} \text{min}^{-1})$	19.20000	8.884000	0.152300	0.331200	-4.788010
	$q_e(\text{mg/g})$	335.7660	52.95520	8.306370	8.588930	7.015340
	$R^2$	0.848051	0.957814	0.878064	0.959352	0.974570

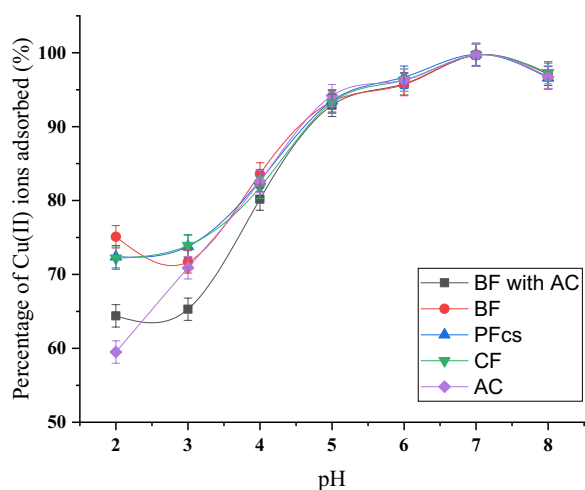


**Fig. 6** Effect of pH on the extent of Cu (II) ions sorption by CWFs

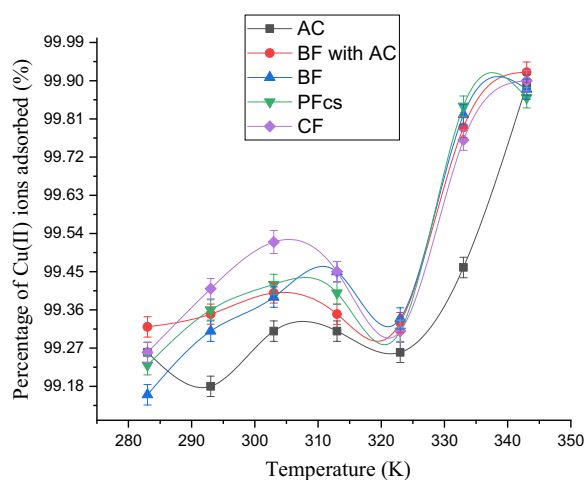


**Fig. 7** A plot of temperature against percentage copper ion uptake by CWF materials

obtained in this study for Cu (II) ions' interaction with CWF adsorbent are negative and larger than  $-40 \text{ kJ/mol}$ , which implies that the mechanism of sorption is predominantly chemisorption.

**Adsorption isotherms of selected CWF materials (BF, PFcs, CF, AC and BF with AC)**

The sorption isotherm suggests how the adsorbed copper (II) ions are distributed between the liquid phase and the CWF materials when equilibrium is established. The analysis of the isotherm data by fitting them to different isotherm models (Table 7) is an important step in finding a suitable model that could be used to describe the process. The extent of Cu (II) ions sorption of CWF materials was studied with the Langmuir, Temkin and Freundlich adsorption isotherms. The Cu (II) ions sorption isotherm of the CWF-adsorbent (AC, BF with AC, BF, PFcs and CF) obey the linearized Freundlich model ( $R^2 > 0.8$  for all adsorbents), as shown in Table 7.

The isotherm data fits the Freundlich model well with  $R^2$  values of 0.883, 0.861, 0.988, 0.866 and 0.959 for AC, BF with AC, BF, PFcs and CF, respectively. The  $K_f$  is the Freundlich isotherm constants, which indicate the adsorption capacity with values of 0.01738, 0.05820, 0.00336, 0.00394 and 0.13113 for AC, BF with AC, BF, PFcs and CF respectively. This indicates that the adsorption capacity for the CWF-adsorbent is in the order  $CF > BF \text{ with AC} > AC > PFcs > BF$ . In addition, the adsorption intensity ( $1/n$ ) of the materials are 1.44691, 1.00805, 1.46828, 1.45494 and 0.90148 for AC, BF with AC, BF, PFcs and CF respectively. This indicates that the adsorption intensity is in the order  $BF > PFcs > AC > BF \text{ with AC} > CF$  suggesting that favorability of the adsorption process. The affinity of the CWF-adsorbent for Cu (II) ions is indicated by the values of  $n$  (Dada et al. 2013). When  $n=1$ , the partition between the two phases is independent of concentration; From Table 7, the affinity of the CWF-adsorbent are CF, BF with AC, AC, PFcs and BF, in the order of strength.

**Table 6** Thermodynamic parameters of uptake of copper ions by CWF composition

CWFs	Ea (kJ/mol)	$\Delta H^\circ$ (kJ/mol)	$\Delta S^\circ$ (kJ/Kmol)	$\Delta G^\circ$ (kJ/mol)						
				283 K	293 K	303 K	313 K	323 K	333 K	343 K
AC	+19.300	+48.210	+0.4330	-74.251	-78.578	-82.905	-87.233	-91.559	-95.887	-100.214
BF with AC	+25.510	+114.220	+0.5740	-48.339	-54.083	-59.828	-65.572	-71.316	-77.059	-82.804
BF	+25.240	+115.650	+0.5760	-47.452	-53.215	-58.979	-64.742	-70.505	-76.269	-82.032
PFcs	+23.040	+101.550	+0.5320	-49.089	-54.412	-59.735	-65.058	-70.381	-75.704	-81.027
CF	+22.150	+91.430	+0.5020	-50.541	-55.557	-60.574	-65.591	-70.607	-75.624	-80.640

**Table 7** Isotherms model parameters for the removal of Cu (II) ions from aqueous solution by CWF compositions

Isotherm models	CWF				
	AC	BF with AC	BF	PFcs	CF
<i>Freundlich</i>					
1/n	1.44691	1.00805	1.46828	1.45494	0.90148
n	0.690	0.990	0.680	0.690	1.109
K <sub>f</sub> (mg/g)	0.01738	0.05820	0.00336	0.00394	0.13113
R <sup>2</sup>	0.88262	0.86132	0.98793	0.86584	0.95995
<i>Langmuir</i>					
b(l/mg)	0.00076	3.77 × 10 <sup>-5</sup>	0.00078	0.00079	0.00026
A <sub>s</sub> (mg/g)	223.705	1585.47	47.6615	50.2982	307.035
R <sup>2</sup>	0.432299	0.00116	0.79761	0.39044	0.16388
<i>Temkin</i>					
A (l/mg)	191.162	138.960	191.013	0.00534	0.00884
B (Kcal/mol)	0.004008	0.0247	0.0186	0.01766	0.02515
dQ	147.753	24.1007	31.8833	33.6427	23.6235
R <sup>2</sup>	0.80928	0.79003	0.99689	0.69123	0.69123

Also, It could be seen from Table 7 that the isotherm data fit the Langmuir equation poorly (R<sup>2</sup>=0.432 for AC, R<sup>2</sup>=0.001 for BF with AC, R<sup>2</sup>=0.798 for BF, R<sup>2</sup>=0.390 for PFcs and R<sup>2</sup>=0.164 for CF) as compared to that of Freundlich and Temkin equations. However, the values of A<sub>s</sub> and b of the Langmuir isotherm was determined from the plot of C<sub>e</sub>/q<sub>e</sub> against C<sub>e</sub> and the values of A<sub>s</sub> and b are noted to be 223.705 and 0.00076 for AC, 1585.47 and 3.77 × 10<sup>-5</sup> for BF with AC, 47.6615 and 0.00078 for BF, 50.2982 and 0.00079 for PFcs and 307.035 and 0.00026 for CF respectively. The values of b of the Langmuir isotherm of all the CWF-adsorbent were low and could suggest that less amount of energy is required for the adsorption of divalent metal ions. This corroborates the activation energy of the CWF-adsorbents as indicated in Table 6. In addition, the large adsorption capacity indicated by BF wuth AC, suggest that the addition of other AC-adsorbent material to the BF-adsorbent increased the Cu (II) adsorption process of the filters.

The values of the Temkin constants A and B as stated in Table 7 were 191.162 l/mg and 16.7683 for AC, 138.960 l/mg and 103.146 for BF with AC, 191.013 l/mg and 77.9682 for BF, 0.00534 l/mg and 73.8909 for PFcs and 0.00884 l/mg and 105.229 for CF. The correlation coefficient of 0.809 for AC, 0.790 for BF with AC, 0.997 for BF, 0.691 for PFcs and 0.691 for CF obtained indicate that the sorption of Cu (II) ions fits the Temkin model. It could be inferred from all three isotherms that the Freundlich model was obeyed better than the Temkin and Langmuir models, as indicated in the values of the regression coefficients (R<sup>2</sup>) for all CWF-adsorbent materials. This suggest that the divalent metal ions adsorption by CWF-adsorbents could not accrue in homogeneous monolayer but a heterogeneous complex way. According to the theory of the Freundlich isotherm model, the heterogeneous surface of the CWF-adsorbents could have different type of adsorption sites, and the affinities of these adsorption sites for divalent metal ions are different.

**Comparative analysis of adsorption during filtration to batch experimental data**

Comparing metal ion uptake of CWF during the filtration process and batch experiments, it could be observed from Fig. 8a, c, that the percentage of copper adsorbed by CF and PFcs at optimum conditions were appreciable (68.9 to 88.8%) during the batch experiment but this was not observed during the filtration process for Fe (II) ions removal, which could be as a result of insufficient contact time and high flow rate (7.5 L/H for PFcs). In the case of BF with AC, divalent metal removal during filtration was appreciable compared to batch experiment data as observed in Fig. 8b. This could be as a result of the low rate of flow (1.3 L/H) of water through the filter material which translates into more contact time between the divalent ions in the solution and the filter material. This indicates that the flow rate directly affects the divalent metal removal efficiency of the CWF materials during water purification processes.. Although, it is worth noting that time is of no consequence, if the mechanism of species removal is weak thus, flow rate is considered an

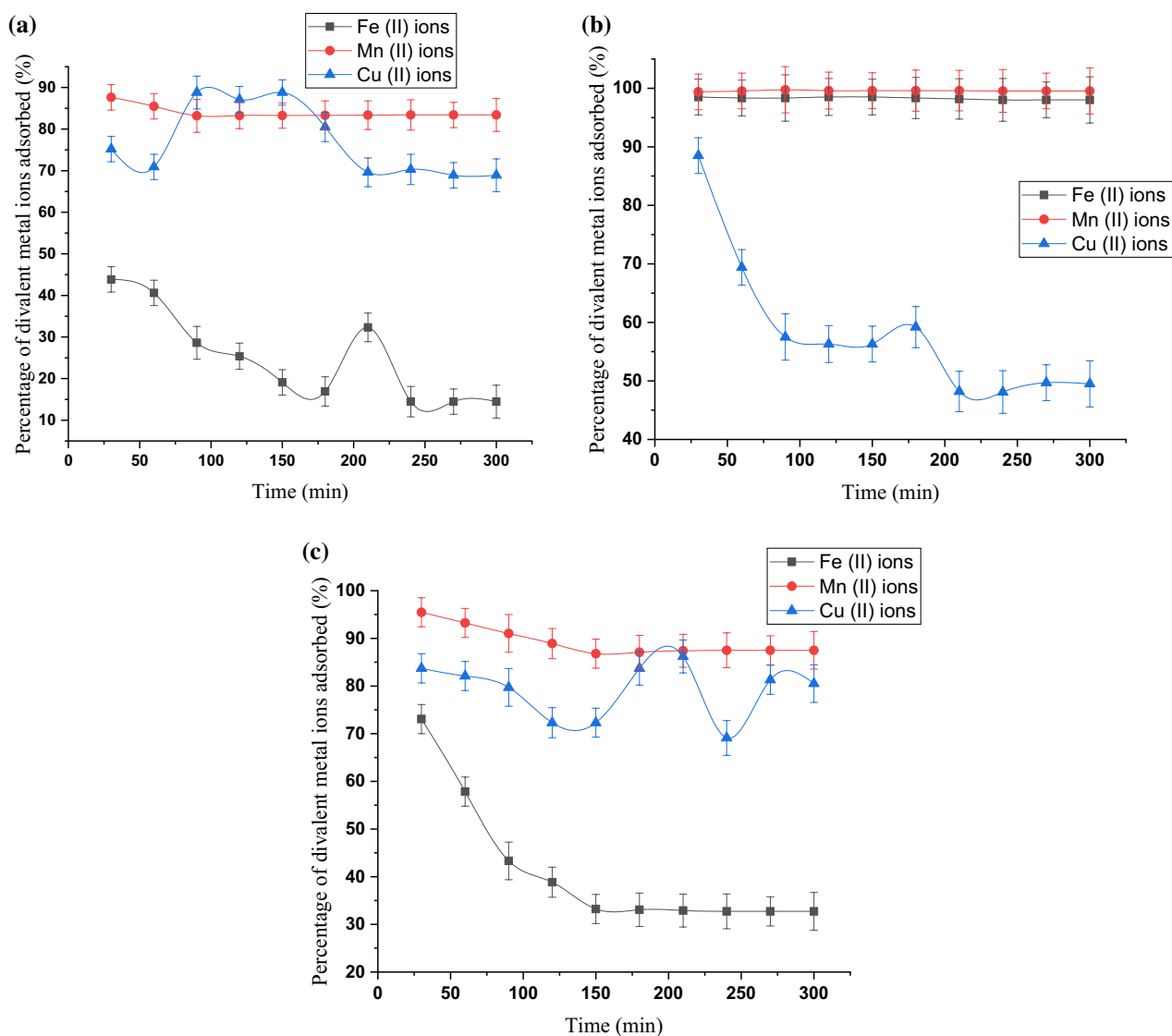


**Fig. 8** A plot of percentage of divalent metal ions adsorbed by **a** PFcs, **b** BF with AC and **c** CF material against time

important variable as a function of efficiency.(i.e., there exists an interaction between sorbate and sorbent).

The assessment of the differences in the amount of divalent metal adsorbed by the pulverized CWF materials against the CWFs during filtration is presented in Table 8.

Further analysis of the paired sample t-test of the amount of divalent metal ions adsorbed during filtration and batch experiments revealed that there is significant difference ( $p \leq 0.00$ ) of the amount of copper

ions adsorbed by the pulverized CWF materials during batched experiments as compared to the filter materials during filtration. This analysis was based on the mass of the filter as compared to mass used in the batch experiments. The observation indicates that the amount of copper (II) ions adsorbed during batch experiment is greater than the amount of other metal ions (manganese (II) and iron (II) ions) adsorbed during filtration experiments (Table 8).

**Table 8** Pairwise sample test for the divalent metal adsorbed during filtration and batch experiment of CWFs

		Paired differences				t	df	Sig. (2-tailed)	
		Mean	Std. deviation	Std. error mean	95% confidence interval of the difference				
					Lower				Upper
Pair 1	Amount of copper ions adsorbed—Amount of manganese ions adsorbed	24.267	28.189	5.528	12.881	35.652	4.390	25	.000
Pair 2	Amount of copper ions adsorbed—Amount of iron ions adsorbed	24.265	28.187	5.528	12.879	35.65021	4.389	25	.000

## Conclusion

Within the limits of the research, from the study, it is evident that the commercially available CWF materials proved to be effective low-cost adsorbents which could remove divalent metal ions in batch and filtration experiments. The adsorption behavior of the pulverized CWF materials indicated that the equilibrium time is 2 h (CF, BF and PF), 90 min (BF with AC) and 40 min (AC). The optimum pH for maximum adsorption is 7 for all CWF materials. The values of  $\Delta H^\circ$  indicated that the Cu (II) ions adsorption process of the CWF adsorbents are endothermic. The processes are best described by the Freundlich isotherm model since the correlation coefficient of all CWF adsorbents is closer to unity. Kinetics studies of the filter materials indicate that the adsorption of CWF adsorbents could be described with the pseudo-second-order model. Based on the kinetics and thermodynamic behavior of the CWF adsorbent, it could be concluded that the mechanism of Cu (II) ions uptake by CWF adsorbents is chemisorption. Comparative analysis of the mass of divalent metal ions (Cu (II), Fe (II) and Mn (II) ions) adsorbed by the CWF materials, indicates that adsorption of divalent metal ions during batch experiment is significant ( $p \leq 0.00$ ) as compared to the amount adsorbed during membrane filtration. The study noted that with enough contact time during filtration processes, the CWF materials could be efficient in metal ion removal. This suggests that the flow rate of the system is a function of the metal removability (KD) of the filter material. Therefore, CWF manufacturers should consider the rate of filtration as a vital parameter during production.

## Acknowledgements

The Authors are grateful to the Ghana Water Company Limited Northern Regional laboratory, Tamale, for the permission to use the laboratory facility of the company for the water quality analyses. Also, we thank the management and staff of C. K. Tedam University of Technology and Applied Sciences, Applied Chemistry Department for the use of the chemistry laboratory and the inputs made by colleagues during the seminar sessions.

## Author contributions

The research Idea was by OBA and BEA. The experiments were conducted by BEA under the supervision of OBA and BA. The manuscript was written by BEA and OBA, and reviewed by BA and EOO.

## Funding

This research did not receive any funding. All financial commitments were borne by the authors in full.

## Availability of data and materials

The data generated during the research are with the corresponding author and may be made available upon request.

## Declarations

### Ethics approval and consent to participate

Not applicable.

### Consent for publication

Not applicable.

### Competing interests

There are no competing interests of financial or personal nature.

Received: 24 August 2023 Accepted: 2 November 2023

Published online: 15 November 2023

## References

- Abdullayev A, Bekheet MF, Hanaor DAH, Gurlo A (2019) Materials and applications for low-cost ceramic membranes. *Membranes* 9(105):1–31
- Ajayi BA, Lamidi YD (2015) Formulation of ceramic water filter composition for the treatment of heavy metals and correction of physiochemical parameters in household water. *Art Design Rev* 3:94–100
- Akosile SI, Ajibade FO, Lasisi KH, Ajibade TF, Adewumi JR, Babatola JO, Oguntuase AM (2020) Performance evaluation of locally produced ceramic filters for household water treatment in Nigeria. *Sci Afr.* <https://doi.org/10.1016/j.sciaf.2019.e00218>
- Albrecht, T. W. J., Addai-Mensah, J., & Fornasiero, D. (2011). Effect of pH, Concentration and Temperature on Copper and Zinc Hydroxide Formation/Precipitation in Solution. *CHEMECA 2011 - "Engineering a Better World,"* 1–10. <https://pdfs.semanticscholar.org/6ae0/a349aea2ddfb5d1fcd34ff92bff180d5b15f.pdf>
- Aliyu A, Usman MM, Audu N (2019) Development of ceramic disc water filter for domestic use. *Int J Eng Tech Res* 17(5):176–189
- Allwar A et al (2008) Textural characteristics of activated carbons prepared from oil palm shells activated with ZnCl<sub>2</sub> and pyrolysis under nitrogen and carbon dioxide. *J Phys Sci* 19(2):93–104

- Apea OB, Akorley EB, Oyelude EO, Ampadu B (2023) Chemical analysis and filtration efficiency of ceramic point-of-use water filters. *Heliyon* 9(7):1–15. <https://doi.org/10.1016/j.heliyon.2023.e18343>
- Atkins PW (1995) Physical chemistry, 5th edn. Oxford University Press, Oxford
- Bisaba AW (2015) Assessment of the effect of insoluble fiber on nutrient availability during digestion in humans: modelling the absorption propensity of metal nutrient in solution. University for Development Studies.
- Bulta AL, Micheal GAW (2019) Evaluation of the efficiency of ceramic filters for water treatment in Kambata Tabaro zone, southern Ethiopia. *Environ Syst Res* 8(1):1–15. <https://doi.org/10.1186/s40068-018-0129-6>
- Chai JB, Au PI, Mubarak NM, Khalid M, Ng WP, Jagadish P, Walvekar R, Abdullah EC (2020) Adsorption of heavy metal from industrial wastewater onto low-cost Malaysian kaolin clay – based adsorbent. *Environ Sci Pollut Res* 27:13949–13962
- Chaukura N, Chiworeso R, Gwenzi W, Motsa MM, Munzeiwa W, Moyo W, Chikunhe I, Nkambule TT (2020) A new generation low-cost biochar-clay composite 'biscuit' ceramic filter for point-of-use water treatment. *Appl Clay Sci*. <https://doi.org/10.1016/j.clay.2019.105409>
- Coleman CK, Mai E, Miller M, Sharma S, Williamson C, Oza H, Holmes E, Lamer M, Ly C, Stewart J, Sobsey MD (2021) Chitosan coagulation pretreatment to enhance ceramic water filtration for household water treatment. *Int J Mol Sci*. <https://doi.org/10.3390/ijms22189736>
- Dada AO, Ojediran JO, Olalekan AP (2013) Sorption of Pb<sup>2+</sup> from aqueous solution onto modified rice husk: isotherm studies. *Adv Chem Phys* 9:103
- Dan Y, Xu L, Qiang Z, Dong H, Shi H (2021) Chemosphere Preparation of green biosorbent using rice hull to preconcentrate, remove and recover heavy metal and other metal elements from water. *Chemosphere* 262:127940. <https://doi.org/10.1016/j.chemosphere.2020.127940>
- Demirbas A, Pehlivan E, Gode F, Altun T, Arslan G (2005) Adsorption of Cu(II), Zn(II), Ni(II), Pb(II), and Cd(II) from aqueous solution on Amberlite IR-120 synthetic resin. *J Colloid Interface Sci* 282(1):20–25. <https://doi.org/10.1016/j.jcis.2004.08.147>
- Edebali S, Pehlivan E (2014) Evaluation of Cr(III) by ion-exchange resins from aqueous solution: equilibrium, thermodynamics and kinetics. *Desalin Water Treat* 52(37–39):7143–7153. <https://doi.org/10.1080/19443994.2013.821631>
- Erhuanga E, Bolaji Kashim I, Lawrence Akinbogun T (2014) Development of ceramic filters for household water treatment in Nigeria. *Art Design Rev* 02(01):6–10. <https://doi.org/10.4236/adr.2014.21002>
- Fahmi MR, Najib NWAZ, Ping PC, Hamidin N (2011) Mechanism of turbidity and hardness removal in hard water sources by using Moringa oleifera. *J Appl Sci* 11(16):2947–2953. <https://doi.org/10.3923/jas.2011.2947.2953>
- Gu S, Kang X, Wang L, Lichtfouse E, Wang C (2019) Clay mineral adsorbents for heavy metal removal from wastewater: a review. *Environ Chem Lett* 17(2):629–654. <https://doi.org/10.1007/s10311-018-0813-9>
- Gupta M, Gupta H, Kharat DS (2018) Adsorption of Cu(II) by low cost adsorbents and the cost analysis. *Environ Technol Innov* 10:91–101. <https://doi.org/10.1016/j.eti.2018.02.003>
- Horsfall M, Spiiff AI, Abia AA (2004) Studies on the influence of mercaptoacetic acid (MAA) modification of cassava (*Manihot sculenta* Cranz) waste biomass on the adsorption of Cu<sup>2+</sup> and Cd<sup>2+</sup> from aqueous solution. *Bull Korean Chem Soc* 25(7):969–976. <https://doi.org/10.5012/bkcs.2004.25.7.969>
- Hussain TS, Al-Fatlawi AH (2020) Remove chemical contaminants from potable water by household water treatment system. *Civil Eng J* 6(8):1534–1546. <https://doi.org/10.28991/cej-2020-03091565>
- Ismadji S, Soetaredjo FE, Ayucitra A (2015) Natural clay minerals as environmental cleaning agents. [https://doi.org/10.1007/978-3-319-16712-1\\_2](https://doi.org/10.1007/978-3-319-16712-1_2)
- Kalebaila KK, Maseka KJ, Mbulo M (2018) Selected adsorbents for removal of contaminants from wastewater: towards engineering clay minerals. *Open J Appl Sci* 08:355–369. <https://doi.org/10.4236/ojapps.2018.88027>
- Karikari AY, Ansa-Asare OD (2006) Physico-chemical and microbial water quality assessment of Densu river of Ghana. *West Afr J Appl Ecol* 10:87–100
- Kumar SP, Ramakrishnan K, Kirupha DS, Sivanesan S (2010) Thermodynamic and kinetic studies of cadmium adsorption from aqueous solution onto rice husk. *Braz J Chem Eng* 27(2):347–355. <https://doi.org/10.1590/S0104-66322010000200013>
- Madela M, Skuza M (2021) Towards a circular economy : analysis of the use of biowaste as biosorbent for the removal of heavy metals. *Energies* 14(5427):1–16
- Meez E, Rahdar A, Kyzas GZ (2021) Sawdust for the removal of heavy metals from water : a review. *Molecules* 26(4318):1–21
- Mohamed RR (2021) Chitin and chitosan as adsorbents. In: *Natural Polymers-Based Green Adsorbents for Water Treatment*, Elsevier. pp 73–91. <https://doi.org/10.1016/b978-0-12-820541-9.00004-1>
- Momina SM, Isamil S (2018) Regeneration performance of clay-based adsorbents for the removal of industrial dyes: a review. *RSC Adv* 8(43):24571–24587. <https://doi.org/10.1039/c8ra04290j>
- Nabieh KA, Mortada WI, Helmy TE, Kenawy IMM, El-reash YGA (2021) Heliyon Chemically modi fried rice husk as an effective adsorbent for removal of palladium ions. *Heliyon* 7:1–9. <https://doi.org/10.1016/j.heliyon.2021.e06062>
- Naiya TK, Chowdhury P, Bhattacharya AK, Das SK (2009) Saw dust and neem bark as low-cost natural biosorbent for adsorptive removal of Zn(II) and Cd(II) ions from aqueous solutions. *Chem Eng J* 148(1):68–79. <https://doi.org/10.1016/j.cej.2008.08.002>
- Nandi BK, Goswami A, Das AK, Mondal B, Purkait MK (2008) Kinetic and equilibrium studies on the adsorption of crystal violet dye using Kaolin as an adsorbent. *Sep Sci Technol* 43(6):1382–1403. <https://doi.org/10.1080/01496390701885331>
- Nawang R, Zobir M, Amin K (2019) Physicochemical properties of hydroxyapatite/montmorillonite nanocomposite prepared by powder sintering. *Results Phys* 15(102540):1–19. <https://doi.org/10.1016/j.rinp.2019.102540>
- Nayak SP, Singh BK (2007) Instrumental characterization of clay by XRF, XRD and FTIR. *Int J Environ Stud* 30(3):235–238. <https://doi.org/10.1080/00207233.2011.565947>
- Ndebele N, Edokpayi JN, Odiyo JO, Smith JA (2021) Field investigation and economic benefit of a novel method of silver application to ceramic water filters for point-of-use water treatment in low-income settings. *Water*. <https://doi.org/10.3390/w13030285>
- Netti H, Saragih M, Mawarni H (2019) Study of making clay-based ceramic membranes with additional rice husk and sawdust to reduce water turbidity. *Int Conf Nat Resour Technol*. <https://doi.org/10.5220/0008547801380146>
- Otunola BO, Lolade OO (2020) Environmental Technology & Innovation A review on the application of clay minerals as heavy metal adsorbents for remediation purposes. *Environ Technol Innov* 18(100692):1–14. <https://doi.org/10.1016/j.eti.2020.100692>
- Priya AK, Yogeshwaran V, Rajendran S, Hoang TKA, Soto-moscoso M, Ghfar AA, Bathula C (2022) Investigation of mechanism of heavy metals (Cr<sup>6+</sup>, Pb<sup>2+</sup> & Zn<sup>2+</sup>) adsorption from aqueous medium using rice husk ash : Kinetic and thermodynamic approach. *Chemosphere* 286(131796):1–11
- Saha P, Chowdhury S. (2011) Insight into adsorption thermodynamics. (T. Prof. Mizutani, Ed.). Rijeka: InTech. [www.intechopen.com/book/thermodynamics/insight-into-adsorption-thermodynamics](http://www.intechopen.com/book/thermodynamics/insight-into-adsorption-thermodynamics)
- Sanka PM, Rwiza MJ, Mtei KM (2020) Removal of selected heavy metal ions from industrial wastewater using rice and corn husk biochar. *Water Air Soil Pollut* 231(244):1–13
- Shah KA, Joshi GS (2017) Evaluation of water quality index for River Sabarmati, Gujarat. *Appl Water Sci* 7(3):1349–1358. <https://doi.org/10.1007/s13201-015-0318-7>
- Shepard Z, Oyanedel-Craver V (2022) A review of the impact of testing conditions on the performance and quality control of locally manufactured, point-of-use ceramic water filters. *Environ Sci Water Res* 8:510–522
- Uddin MK (2017) A review on the adsorption of heavy metals by clay minerals, with special focus on the past decade. *Chem Eng J* 308:438–462. <https://doi.org/10.1016/j.cej.2016.09.029>
- Whelan MJ, Linstead C, Worrall F, Ormerod SJ, Durance I, Johnson AC, Johnson D, Owen M, Wiik E, Howden NJ, Burt TP (2022) Is water quality in British rivers "better than at any time since the end of the Industrial Revolution"? *Sci Total Environ*. <https://doi.org/10.1016/j.scitotenv.2022.157014>
- WHO (2011) WHO guidelines for drinking-water quality (fourth). WHO Library, Geneva. [https://doi.org/10.1016/S1462-0758\(00\)00006-6](https://doi.org/10.1016/S1462-0758(00)00006-6)
- WHO (2017) Progress on drinking water, sanitation and hygiene 2017 update and SDG baseline. Switzerland.

Wong YC, Szeto YS, Cheung WH, McKay G (2003) Equilibrium studies for acid dye adsorption onto chitosan. *Langmuir* 19(19):7888–7894. <https://doi.org/10.1021/la030064y>

Yang H, Xu S, Chitwood DE, Wang Y (2020) Ceramic water filter for point-of-use water treatment in developing countries: Principles, challenges and opportunities. *Front Environ Sci Eng* 14(5):1–10

### **Publisher's Note**

Springer Nature remains neutral with regard to jurisdictional claims in published maps and institutional affiliations.

**Submit your manuscript to a SpringerOpen<sup>®</sup> journal and benefit from:**

- ▶ Convenient online submission
- ▶ Rigorous peer review
- ▶ Open access: articles freely available online
- ▶ High visibility within the field
- ▶ Retaining the copyright to your article

---

Submit your next manuscript at ▶ [springeropen.com](https://www.springeropen.com)

---